

Reports

Aeromagnetic and Radio Echo Ice-Sounding Measurements Show Much Greater Area of the Dufek Intrusion, Antarctica

Abstract. *A combined aeromagnetic and radio echo ice-sounding survey made in 1978 in Antarctica over the Dufek layered mafic intrusion suggests a minimum area of the intrusion of about 50,000 square kilometers, making it comparable in size with the Bushveld Complex of Africa. Comparisons of the magnetic and subglacial topographic profiles illustrate the usefulness of this combination of methods in studying bedrock geology beneath ice-covered areas. Magnetic anomalies range in peak-to-trough amplitude from about 50 nanoteslas over the lowermost exposed portion of the section in the Dufek Massif to about 3600 nanoteslas over the uppermost part of the section in the Forrestral Range. Theoretical magnetic anomalies, computed from a model based on the subice topography fitted to the highest amplitude observed magnetic anomalies, required normal and reversed magnetizations ranging from 10^{-3} to 10^{-2} electromagnetic units per cubic centimeter. This result is interpreted as indicating that the Dufek intrusion cooled through the Curie isotherm during one or more reversals of the earth's magnetic field.*

The Dufek layered mafic intrusion is the second largest (or possibly the largest) intrusion in the world and has remarkable chemical variation and perfection of layering. Other bodies of this type, especially the Bushveld Complex of South Africa, are valuable sources of ores (1), but if the Dufek intrusion contains ore-type minerals, they will not be exploitable for a number of decades because of the difficulty of access and severe environmental problems that any expedition might cause. Exposed rocks of the intrusion occur in only about 3 percent of its area, which we report here as being at least 50,000 km².

The Dufek intrusion has been under study since 1957 by U.S. geologists (2) and geophysicists (3-5), and a geological-geophysical team from the Soviet Union investigated the area in 1978 (6). The intrusion extends across the transition from West to East Antarctica along the Transantarctic Mountains, of which the Dufek Massif and Forrestral Range are a part (Fig. 1). Before the present study, the minimum area of the intrusion was estimated at 34,000 km² based on gravity and magnetic surveys (3). It is of Jurassic age, horizontally stratified, probably 8 to 9 km thick (3), and dips to the east at a low angle. About 1.7 km of the upper part of the section crops out in the Forrestral Range, and 1.8 km of the lower section is exposed in the Dufek

Massif. About 2 to 3 km of unexposed section is inferred (2, 3) to lie beneath the ice between the ranges, with a second section of 2 to 3 km (3) probably lying hidden beneath the lowest exposed rock layer of the Dufek Massif. The stratigraphy of the Dufek intrusion shows a differentiation trend similar to that of other major layered intrusions. The mafic index (2), density (7), and remanent magnetization and susceptibility (8) increase upward in the section and are correlated with the amplitudes of magnetic anomalies.

Potassium-argon dates of 172 ± 4 million years on several samples (9) are within the range (163 to 179 million years) measured for diabase of the Ferrar Group in the central Transantarctic Mountains (2). Behrendt *et al.* (3) suggested that the Dufek intrusion was related to the rifting of Africa and Antarctica. Ford and Kistler (9) interpreted the Ferrar Group and the Dufek intrusion as evidence of a failed rift along the Transantarctic Mountains at the time of the initial rifting of Africa and Antarctica. They inferred that the Dufek intrusion marks the location of a triple junction that existed at the time of its origin. This would account for the great area of the Dufek intrusion.

During December 1978 we made three flights (a total distance of 4200 km) over the area of the Dufek intrusion, measur-

ing the total magnetic intensity and making radio echo soundings of ice thickness continuously (10). The aircraft operated out of McMurdo, 2200 km from the project area, and refueled at the South Pole.

Aeromagnetic measurements were used extensively in Antarctica in the late 1950's and 1960's (3, 5), and long-range radio echo ice-soundings have been made since 1967 under a cooperative program between the U.S. Antarctica Research Program and the Scott Polar Research Institute (11). However, results of studies in which the two methods were used in combination have not been reported. The objective of the ice-sounding over the Dufek intrusion was the comparison of the bedrock topography with magnetic profiles to obtain a quantitative estimate of rock magnetization and to determine the areal extent of the Dufek intrusion. The aircraft flew at an elevation of about 2 km above sea level over the mountains and grounded ice and 1 km above sea level over the ice shelf, but some departures from these levels were required by the topographic clearance requirements of the aircraft.

Figure 1 shows the magnetic profiles we obtained. Anomaly amplitudes observed a few hundred meters above outcrops of the intrusion ranged from 3600 nT over the Forrestral Range to 50 nT over the Dufek Massif. The extension of the anomalies north of the ranges over the Ronne Ice Shelf and southeast of the Forrestral Range is apparent. The bedrock surface is about 1.7 km below sea level (minimum depth to the top of the intrusion) beneath the Ronne Ice Shelf (12), 2.3 km above sea level over the highest peaks of the Dufek Massif, and about 2 km below sea level beneath the Support Force Glacier. Therefore, anomaly amplitudes are lower over the ice shelf and the thick ice-covered areas east of the Forrestral Range.

We plotted the magnetic intensity over the bedrock topography on four typical profiles (Fig. 2A). Note both the positive correlation (for example, line 26) and the negative correlation (for example, line 24) of topography and anomaly amplitude, which are inferred to be the result of normal and reversed magnetization, respectively; these two lines cross the ridge about 15 km apart. Measured susceptibility ranges from 0.1 to 0.0007 emu/cm³, and normal and reversed remanent magnetization ranges from 0.1 to 0.0006 emu/cm³ (13) from the top of the section to its lowest part ($1.3 < Q < 5$, where Q is the ratio of remanent magnetization to induced magnetization). The present field direction lies within the scatter of

points for the measured direction of remanent magnetization (8), so that in the calculated anomalies discussed below, it is reasonable to assume a direction of magnetization in the present field direction with either a normal or reversed polarization.

In Fig. 2A, the profiles for line 24 show no anomalies over the Paleozoic sedimentary rocks (3) of the Cordiner Peaks. The magnetic profile is plotted on line 33

on two scales, amplifying the anomalies east and west of the Forrestal Range. We interpret the source of the anomalies of 100 to 200 nT as being the buried portion of the Dufek intrusion. This is consistent with computer models (magnetizations, about 0.001 to 0.004 emu/cm³) and is within the range of magnetizations required to fit the high-amplitude anomalies over the Dufek Massif and Forrestal Ranges (Fig. 2B). Note the absence of

magnetic anomalies over the sedimentary rocks thought to compose the subglacial mountain range shown at the right end of line 23 in Fig. 2A. We infer that the Dufek intrusion also causes the low-amplitude anomalies shown on lines D, 31, 65-36, and 65-37 near those southeast of the Forrestal Range on line 23.

The approximately 2-km vertical relief between the bedrock southeast of the Support Force Glacier and the moun-

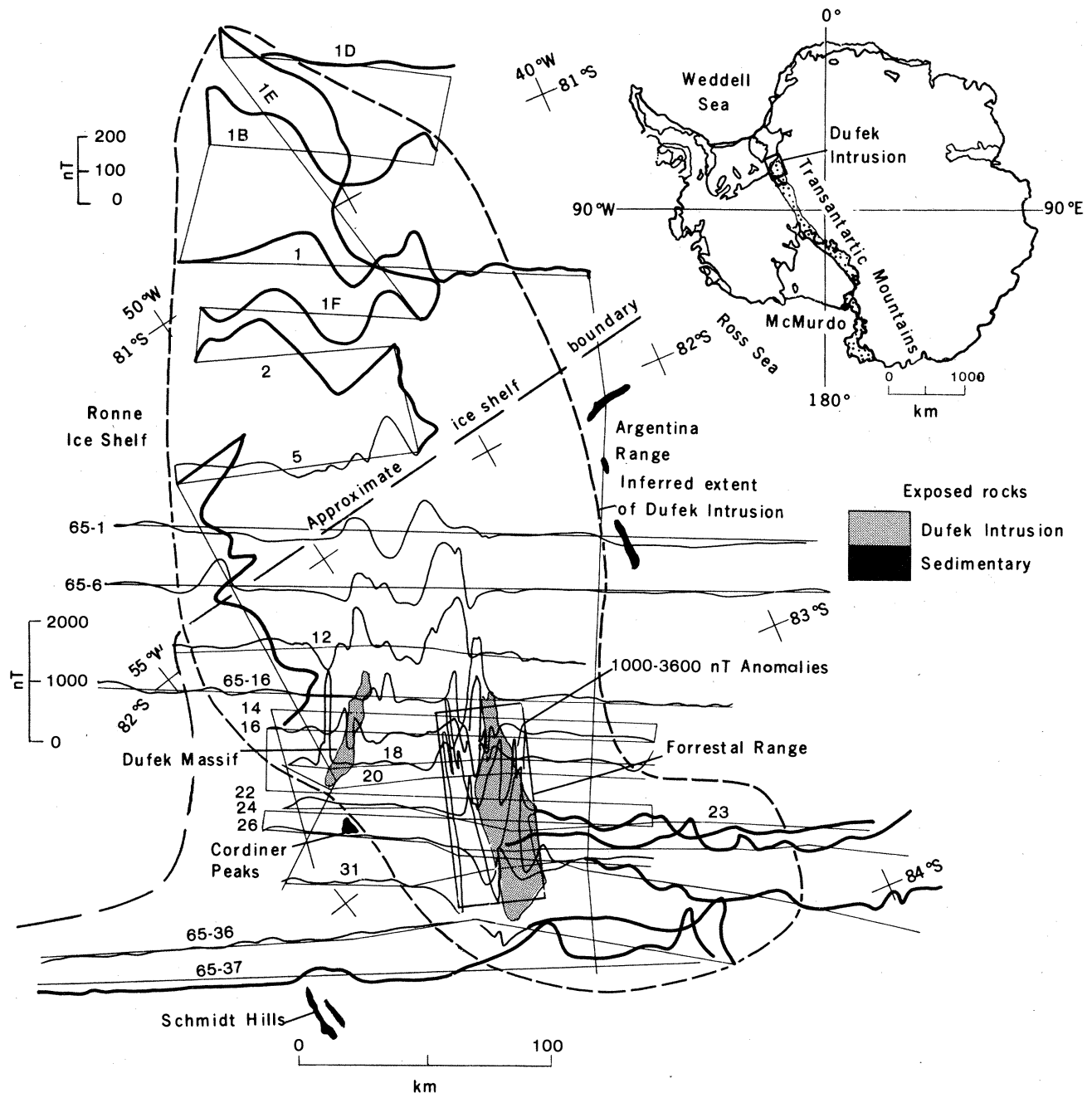


Fig. 1. Aeromagnetic profiles superimposed on a map showing line locations. Note that anomalies north of line 5 over the Ronne Ice Shelf and southeast of the Forrestal Range are plotted with a heavier line drawn at a magnified scale relative to the rest. Anomalies on lines 14, 20, 22, and 24 are omitted because of the confusion of the high-amplitude anomalies over the ranges. The continuation of the anomaly trends from the outcrops of the Dufek intrusion in the Forrestal Range and Dufek Massif north over the Ronne Ice Shelf is apparent. (The high-amplitude anomalies over the Forrestal Range are better illustrated in Fig. 2A.) Profiles 65-1, 65-6, 65-36, and 65-37 are from an earlier survey (3). Note the small area of outcrops of the Dufek intrusion compared with the extent of the intrusion inferred from the magnetic, gravity, and radio echo ice-sounding data.

tains of the Dufek Massif and Forrestal Range (Fig. 2A) suggests a major fault along the southeast margin of the Forrestal Range. A fault with approximately 4 km of vertical displacement, which was previously interpreted as bounding the northern ends of these two ranges (3), accounts for the lower amplitudes of the magnetic anomalies observed over the Ronne Ice Shelf.

We computed a model in which theoretical magnetic anomalies were fitted to the observed magnetic field along line 12, just north of the ranges (Fig. 2B). The topography measured along the radar reflection profile was used to define the top of the model, and remanent magnetizations in the present field direction

(both normal and reversed) were solved by Cady's (14) inversion method. Because the magnetizations in the Dufek intrusion decrease with depth by three to four orders of magnitude (8, 13), the higher layers (stratigraphically, topographically, and magnetically) mask those beneath. Therefore, in computing our models for the higher amplitude magnetic anomalies, we largely ignored the layers beneath. The model dips to the southeast at a low angle, which is consistent with stratigraphic measurements (2). Magnetizations up to 0.05 emu/cm³ were required in the present field direction. The model suggests alternately interbedded normal and reversed magnetizations that are probably the re-

sult of cooling of the original intrusion through the Curie isotherms during at least one polarity reversal [as discussed by Beck (8) on the basis of oriented samples]. Erosion and displacement of normally or reversely magnetized units by faulting probably account for the complexity of the magnetic field shown by the magnetic profiles in Figs. 1 and 2.

We used our findings to outline the approximate minimum areal extent of the Dufek intrusion (Fig. 1). We included the anomalies over the Ronne Ice Shelf on trend with those over the Dufek Massif and Forrestal Range. In the area between lines 1 and 65-1, we assumed continuity at their east ends because of the anomalies indicated near the dashed line. South of line 18, the dashed line was drawn at the southeast to include the anomalies indicated.

A positive Bouguer anomaly over the intrusion, 50 to 60 cm/sec², occurs superimposed on the gradient from 100 to -90 cm/sec² across the front of the Transantarctic Mountains from West to East Antarctica (3). On the basis of a single seismic ice-sounding and gravity observation, the positive Bouguer anomaly associated with the Dufek intrusion was previously inferred to extend to 83°34'S, 45°09'W (3). A flight was made along line D (Fig. 2) in order to cross a number of the locations of gravity observations at which only free-air anomalies had been calculated (3) because of the lack of ice-thickness data. Using the measured radio echo ice thicknesses at the gravity stations, we calculated Bouguer anomalies that confirm the existence of the positive gravity anomaly and that support the location of the boundary indicated in Fig. 1.

We estimate that the area of the Dufek intrusion is about 50,000 km². This compares with 66,000 km² reported for the Bushveld Complex, the largest yet identified on the earth (1). Additional surveys north and east of our lines might be expected to reveal that the Dufek intrusion has a still greater extent. For example, Behrendt *et al.* (3) found an anomaly, about 900 nT in amplitude at 79°45'S, 45°W that might be caused by the Dufek intrusion.

JOHN C. BEHRENDT

U.S. Geological Survey,
Denver, Colorado 80225

DAVID J. DREWRY

EDWARD JANKOWSKI

Scott Polar Research Institute,

Cambridge University,

Cambridge, CB2 1ER England

MURIEL S. GRIM

U.S. Geological Survey,

Denver 80225

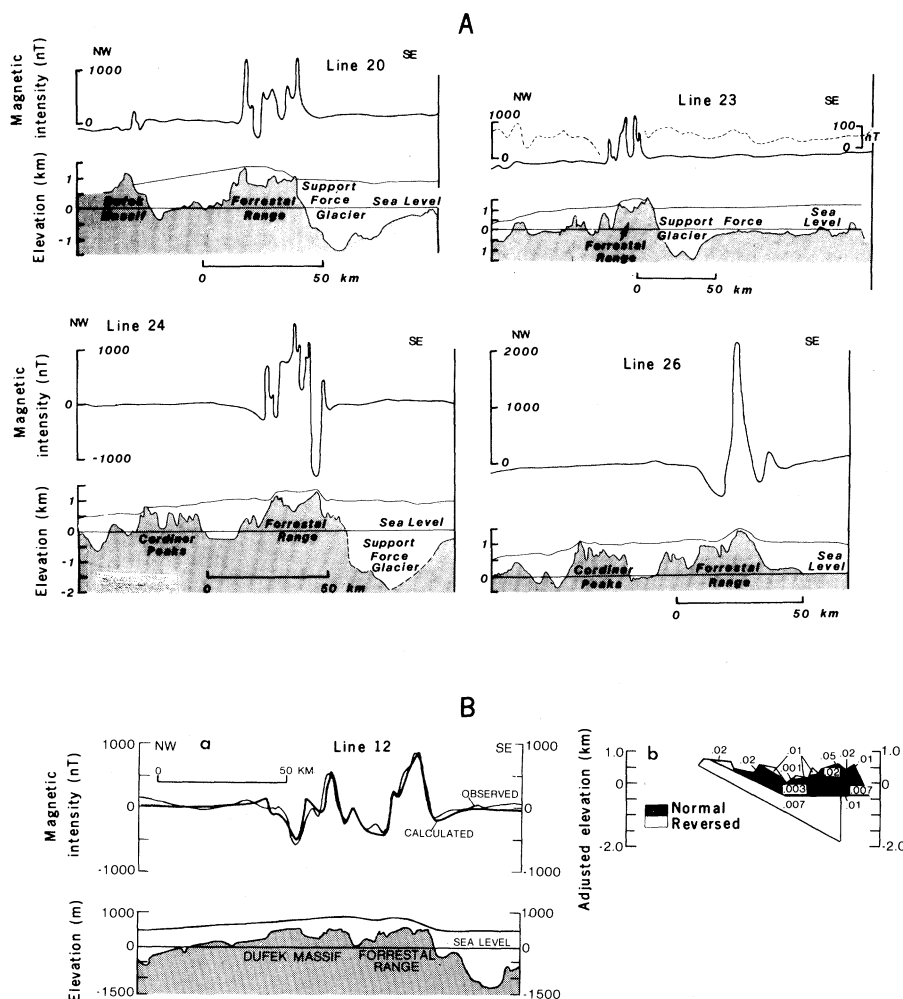


Fig. 2. (A) Aeromagnetic and radio ice-sounding profiles of four typical lines. The vertical exaggeration is 12.5:1. White areas represent ice; shaded areas, rock. Compare the negative anomaly over the ridge of the Forrestal Range on line 24 with the positive anomaly over the ridge on line 26. The magnetic profile northwest and southeast of the Forrestal Range on line 23 is shown at an amplified scale (see the dashed line and the scale at the right end of the profile). (B) Aeromagnetic and radio echo ice-sounding profile along line 12 showing (a) the theoretical anomalies calculated to fit the observed magnetic profile and (b) the model on which they are based. The vertical exaggeration is 12.5:1. Normal and reversed magnetizations are shown in electromagnetic units per cubic centimeter. The top of the model was determined by using the bedrock topography interpreted from the radar ice-sounding profile. Present field direction was based on directions measured from oriented samples (7). The magnetizations and polarities were determined by least-squares fits to the observed profile, and are in the same range as that of measured magnetizations (5, 7). Dips of the magnetic strata are consistent with field observations (2).

References and Notes

1. D. Hunter, *Am. Sci.* **66**, 551 (1978).
2. A. R. Ford, *U.S. Geol. Surv. Bull.* **1405 D** (1976), p. 35; _____, D. L. Schmidt, W. W. Boyd, Jr., *U.S. Geol. Surv. Map A-10* (1978).
3. J. C. Behrendt, J. R. Henderson, L. Meister, W. L. Rambo, *U.S. Geol. Surv. Prof. Pap.* **844** (1974).
4. J. C. Behrendt, L. Meister, J. R. Henderson, *Science* **153**, 1373 (1966).
5. J. C. Behrendt, *ibid.* **144**, 993 (1964); _____ and C. R. Bentley, *Antarctic Map Folio Series Folio 9* (American Geographical Society, New York, 1978).
6. G. Grikurov, personal communication.
7. A. B. Ford and S. W. Nelson, *Antarct. J. U.S.* **7**, 147 (1972).
8. M. E. Beck, Jr., *Geophys. J. R. Astron. Soc.* **28**, 49 (1972).
9. A. B. Ford and R. W. Kistler, *N.Z. J. Geol. Geophys.*, in press.
10. We used a proton precession magnetometer operated by Applied Physics Laboratory, Johns Hopkins University, in a C-130 aircraft owned by the NSF and operated by the U.S. Navy. Ice sounding was done with equipment owned and operated by the Scott Polar Research Institute and the Technical University of Denmark. An inertial navigation system was used for positioning, with guidance provided by USGS topographic maps of the area.
11. D. J. Drewry, *Polar Rec.* **17**, 359 (1975).
12. J. C. Behrendt, *J. Geophys. Res.* **67**, 221 (1962).
13. M. E. Beck, Jr., A. B. Ford, W. W. Boyd, Jr., *Nature (London)* **217**, 534 (1968).
14. J. W. Cady, *Geophysics*, in press.
15. We thank the personnel of U.S. Navy Squadron VXE6 for making flights under arduous and hazardous conditions. The work was supported by an NSF grant to the USGS and by a National Environmental Research Council (United Kingdom) grant to the Scott Polar Research Institute. A. W. England and R. W. Simpson provided valuable discussions, D. J. Meldrum and F. Sondergaard played vital roles in the radio sounding operation, and J. Williams assisted in the compilation and analysis of the data. This report was approved for publication by the director of the U.S. Geological Survey.

29 January 1980; revised 2 April 1980

Gonadal Steroids: Effects on Excitability of Hippocampal Pyramidal Cells

Abstract. *Electrophysiological field potentials from hippocampal slices of rat brain show sex-linked differences in response to $1 \times 10^{-10}M$ concentrations of estradiol and testosterone added to the incubation medium. Slices from male rats show increased excitability to estradiol and not to testosterone. Slices from female rats are not affected by estradiol, but slices from female rats in diestrus show increased excitability in response to testosterone whereas slices from females in proestrus show decreased excitability.*

Sex steroids bind to and affect both morphological and functional properties of the hypothalamus and closely related diencephalic structures (1). In the hippocampus, the binding of tritiated estradiol and testosterone does not approach that in diencephalic structures, nor does the hippocampus bind gonadal steroids with the same degree of affinity as it does adrenal corticosteroids (2). Naturally occurring changes in estradiol during the estrous cycle affect the excitability of brain tissue (3), and experimental administration of estradiol (4) and testosterone (5) alters electrical activity in the limbic system.

To further define the effects of gonadal steroids on neuronal excitability in the rodent hippocampus, we applied testosterone and 17β -estradiol to hippocampal slices (6) from female and male rats. Not only was the excitability of hippocampal pyramidal cells affected by these gonadal steroids, but the response profiles were different for hippocampal slices from male and female rats.

Slices of the hippocampus were obtained from adult male and female rats by standard procedures (7). Stage of estrus in females was determined by microscopic analysis of vaginal smears (8). Stimulating electrodes were placed in the Schaffer collateral pathway (see Fig. 1A), which is afferent to the CA1 pyramidal cells, from which field potential re-

sponses were recorded in the cell body layer (9). Figure 1B shows representative monosynaptic field potentials prior to and 20 minutes after steroid administration (10). All measurements of population spike responses (7) obtained after administering steroids were expressed as a percentage of the corresponding control (before steroid administration) value. Responses qualitatively identical to the response at 20 minutes could be observed as soon as 5 minutes after steroid administration. Steroids were added to the media in a concentration of $1 \times 10^{-10}M$ as an aqueous suspension with polyvinylpyrrolidone (11).

The addition of 17β -estradiol and testosterone affected the excitability of the CA1 neurons to suprathreshold afferent stimulation. The steroids had no effect on the population excitatory postsynaptic potential threshold. Hippocampal slices from male rats exposed to estradiol exhibited the greatest change in excitability; the CA1 population spike was increased in amplitude by an average of 72.6 percent. In contrast, a small and inconsistent increase (13.6 percent) in population spike amplitude was observed when slices from male rats were treated with testosterone.

Statistical tests (*t*-test) indicated that the spike amplitudes in slices from male animals given estradiol were reliably higher than those of corresponding slices

treated with testosterone ($P < .05$) and that increases produced by testosterone were not significantly different from those observed in the control experiments. Control experiments with slices from male animals placed in medium either with or without the polyvinylpyrrolidone vehicle yielded no consistent change (12).

When hippocampal slices from diestrous female rats were treated with testosterone, the spike amplitudes increased by an average of 21.7 percent. A consistent slight depression in pyramidal cell population spike amplitude (8.1 percent) was obtained in slices from diestrous animals after administration of estradiol.

In slices from proestrous animals, estradiol produced an insignificant increase (2.3 percent) in the mean amplitude of pyramidal cell responses. A much larger effect was produced by the same concentration of testosterone which attenuated synaptic activity by 22.2 percent in slices from proestrous females. The difference between mean relative amplitudes for slices from diestrous and proestrous animals treated with testosterone was statistically significant ($P < .01$). The results are summarized in Fig. 1C.

These findings may be examined in terms of a classical receptor binding mechanism. In that mechanism, the ability of a steroid hormone to affect cell function depends on an interaction of the steroid with an unoccupied cytosol receptor protein and subsequent migration of the steroid-receptor complex to the nucleus where RNA and protein synthesis may be affected. Separate receptor proteins for estradiol and testosterone have been characterized, with both types of receptor being found in both genders (13). The changes in excitability that we observed in slices from male rats are difficult to attribute to increased protein synthesis resulting from estrogen-triggered new messenger RNA production, since the effects are seen with virtually no lag phase. Moreover, the results obtained for slices from female animals appeared to be independent of stage within the estrous cycle. Since estradiol occurs in highest concentrations during proestrus and lowest during diestrus, the level of endogenous estrogen or free receptor does not seem to be a response-determining factor. We observed no significant response to estradiol in slices from diestrous or proestrous females despite the large effect of this steroid in male tissue. In addition, testosterone was excitatory in slices from diestrous females, but inhibitory in slices from proestrous animals. The changes in excitability produced by both steroids were